

ADAMTS Metalloproteases Generate Active Versican Fragments that Regulate Interdigital Web Regression

Daniel R. McCulloch,¹ Courtney M. Nelson,¹ Laura J. Dixon,¹ Debra L. Silver,² James D. Wylie,¹ Volkhard Lindner,³ Takako Sasaki,⁴ Marion A. Cooley,⁵ W. Scott Argraves,⁵ and Suneel S. Apte^{1,*}

¹Department of Biomedical Engineering, Lerner Research Institute, ND20-Cleveland Clinic, 9500 Euclid Avenue, Cleveland, OH 44195, USA

²Genetic Disease Research Branch, National Human Genome Research Institute, Bethesda, MD 20892, USA

³Maine Medical Center Research Institute, Scarborough, ME 04074, USA

⁴Department of Biochemistry and Molecular Biology, Oregon Health & Science University, Portland, OR 97239, USA

⁵Department of Anatomy and Cell Biology, Medical University of South Carolina, Charleston, SC 29403, USA

*Correspondence: aptes@ccf.org

DOI 10.1016/j.devcel.2009.09.008

SUMMARY

We show that combinatorial mouse alleles for the secreted metalloproteases *Adamts5*, *Adamts20* (*bt*), and *Adamts9* result in fully penetrant soft-tissue syndactyly. Interdigital webs in *Adamts5*^{-/-};*bt/bt* mice had reduced apoptosis and decreased cleavage of the proteoglycan versican; however, the BMP-FGF axis, which regulates interdigital apoptosis was unaffected. BMP4 induced apoptosis, but without concomitant versican proteolysis. Haploinsufficiency of either *Vcan* or *Fbln1*, a cofactor for versican processing by ADAMTS5, led to highly penetrant syndactyly in *bt* mice, suggesting that cleaved versican was essential for web regression. The local application of an aminoterminal versican fragment corresponding to ADAMTS-processed versican, induced cell death in *Adamts5*^{-/-};*bt/bt* webs. Thus, ADAMTS proteases cooperatively maintain versican proteolysis above a required threshold to create a permissive environment for apoptosis. The data highlight the developmental significance of proteolytic action on the ECM, not only as a clearance mechanism, but also as a means to generate bioactive versican fragments.

INTRODUCTION

Classic examples of tissue sculpting during morphogenesis include resorption of tadpole tails and fins during amphibian metamorphosis (Gross and Lapiere, 1962) and regression of the interdigital webs during mammalian limb morphogenesis (Zuzarte-Luis and Hurler, 2002). Web regression is highly regulated, since interdigital tissue (IDT) provides cues for precise development of the skeletal elements of the autopod (Dahn and Fallon, 2000). Persistence of IDT leads to soft-tissue syndactyly (STS) in which only web resorption is affected, and is distinct from osseous syndactyly, where the skeletal elements of adjacent rays are fused owing to anomalous patterning earlier in development. STS is a relatively common developmental anomaly, occurring either in isolation or in association with other defects.

Web regression requires removal of interdigital cells, which occurs by apoptosis, as well as clearance of extracellular matrix (ECM). A complex interplay between BMPs (bone morphogenetic proteins) and FGFs (fibroblast growth factors) mediates apoptosis during IDT regression. During early mouse autopod development, FGFs produced in the apical ectodermal ridge (AER) promote outgrowth and suppress BMP production in the prospective IDT (Boulet et al., 2004; Lu et al., 2006; Weatherbee et al., 2006). BMPs also appear to regulate FGFs, which then act as survival factors for IDT cells (Pajni-Underwood et al., 2007). Once autopod patterning is complete, the AER regresses, FGF production in the AER declines, and BMP expression in the IDT is upregulated, leading to apoptosis of interdigital cells (Ganan et al., 1996; Guha et al., 2002; Merino et al., 1999a, 1999b; Weatherbee et al., 2006). STS is observed in *Bmp*-deficient mice (Bandyopadhyay et al., 2006) and can be induced by the presence of the BMP inhibitor Gremlin (Merino et al., 1999b). Gremlin expression in the bat forelimb and duck hindlimb IDT may be a mechanism that ensures web retention and allows the formation of wings and webbed feet, respectively (Weatherbee et al., 2006; Zou and Niswander, 1996).

In contrast to extensive published work on apoptosis during interdigital web regression, mechanisms for removal of the web ECM have not been previously identified, nor is it understood how synchronous removal of cells and ECM is achieved. During amphibian metamorphosis, the redundant tissues are collagen-rich, and induction of a secreted collagenase, which was incidentally the first discovered matrix-degrading metalloprotease, is necessary (Gross and Lapiere, 1962). However, IDT has an embryonic matrix, containing hyaluronan, proteoglycans, and fibronectin, and collagenase is unlikely to have a major role in its regression. Here, we show that combinations of null alleles for three ADAMTS proteases (*Adamts5*, *Adamts9*, and *Adamts20* (*bt*)) lead to STS, but do not affect skeletal patterning, indicating a temporally and spatially restricted role during web regression. These ADAMTS proteases belong to an evolutionarily related cluster of secreted metalloproteases that share the ability to cleave large aggregating chondroitin-sulfate proteoglycans (Apte, 2009). One such substrate is versican, a widespread embryonic proteoglycan, which forms complexes with hyaluronan through its N-terminal G1 domain (Kimata et al., 1986; Matsumoto et al., 2003) and interacts with several other molecules, including fibulin-1 (Aspberg et al., 1999), through its C-terminal

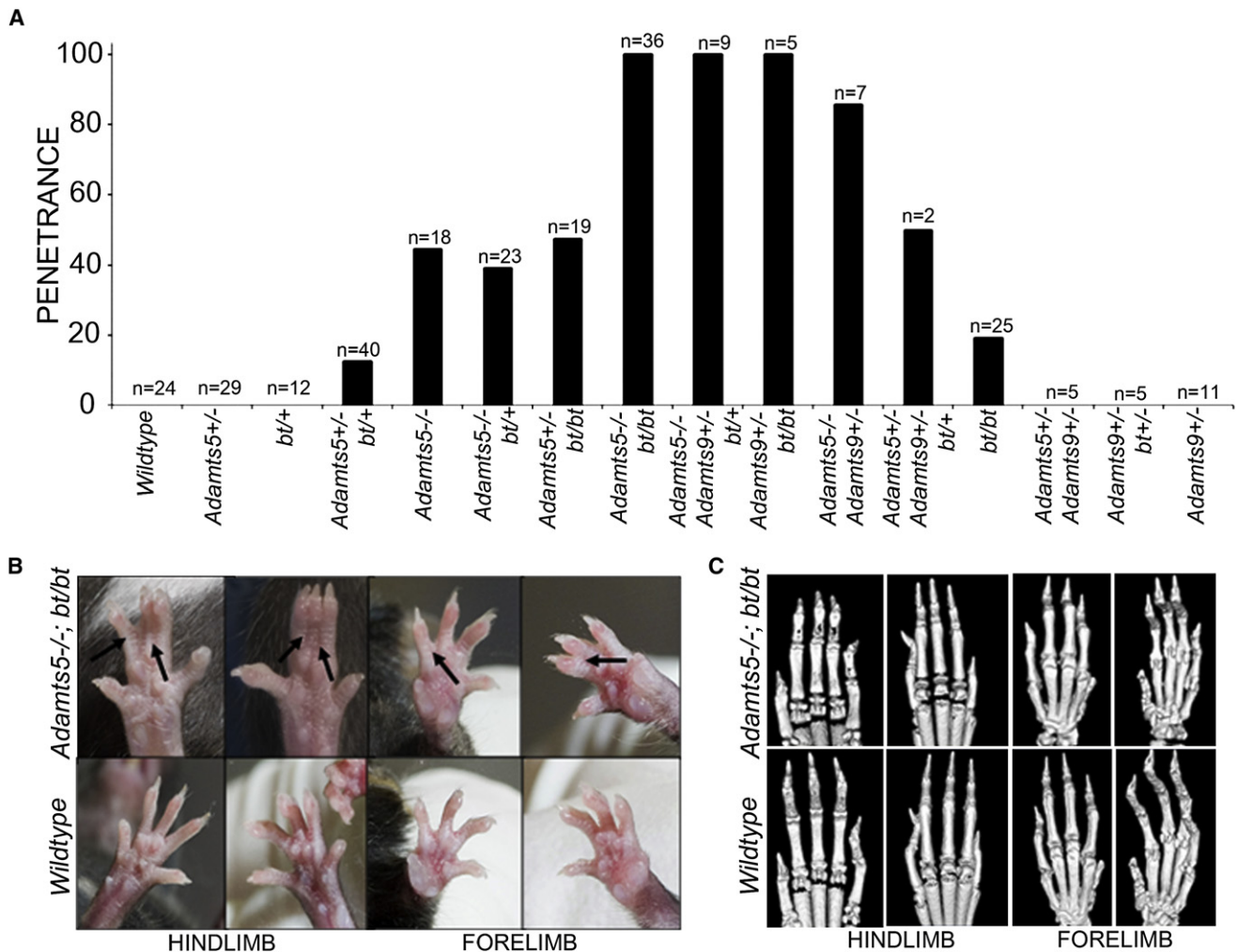


Figure 1. Combinatorial Mutant Adamts Alleles Develop STS with Greater Penetrance than Single Adamts Mutants

(A) Histogram of penetrance of STS in mice of the indicated genotype. The number of mice evaluated for each genotype is indicated above each bar. Note the general trend toward a higher penetrance with increasing dosage of inactivated (*Adamts5*, *Adamts9*) or mutant (*bt*) alleles.

(B) Representative types of STS seen in *Adamts5*^{-/-};bt/bt forelimbs and hindlimbs compared to wild-type limbs. Arrows indicate persistent interdigital webs.

(C) Three-dimensional reconstruction following mCT analysis of 3 week old *Adamts5*^{-/-};bt/bt paws shows normal patterning and no radiological anomalies. Wild-type limbs are shown as controls.

G3 domain. Our findings reveal an operational model in which these ADAMTS proteases work cooperatively to influence apoptosis during web regression through the production of cleaved versican.

RESULTS

Adamts5^{-/-};bt/bt Mice Develop STS with Greater Penetrance than *Adamts5*^{-/-} or bt/bt Mice

In the course of investigating genes that could modify a white spotting defect in ADAMTS20-deficient *bt* mice (Silver et al., 2008), we found that *Adamts5*^{-/-};bt/bt mice developed syndactyly with 100% penetrance (Figure 1A). In contrast, *Adamts5*^{-/-} mice and *bt/bt* mice each had a considerably lower penetrance of syndactyly (44% and 18%, respectively). Penetrance in combinatorial mice was dependent on the dosage of the mutant alleles (Figure 1A). While at least three of four limbs were involved

in each *Adamts5*^{-/-};bt/bt mouse (see Figure S1 available online), the severity and extent of fusion varied (Figure 1B). The IDT between hindlimb digits 3 and 4 was most frequently involved in *Adamts5*^{-/-};bt/bt mice (Figure S2A) and also had the greatest severity of STS (Figure S2B). Hindlimbs were more frequently affected in *Adamts5*^{-/-} mice, whereas forelimbs were more frequently affected in *bt/bt* mice (Figure S2C). Three-dimensional reconstruction of limbs from mature *Adamts5*^{-/-};bt/bt mice using microcomputed tomography (mCT) showed that osseous syndactyly or patterning defects were absent (Figure 1C). Thus, these proteases act locally in the IDT after completion of limb patterning.

Since ADAMTS20 is homologous to ADAMTS9 (Llamazares et al., 2003; Somerville et al., 2003), we tested whether *Adamts9* participated in IDT resorption. *Adamts9*^{-/-} mice die during early gestation (R.P.T. Somerville and S.S.A., unpublished data); hence, *Adamts5*^{-/-}; *Adamts9*^{+/-} mice and *bt/bt*; *Adamts9*^{+/-}

mice were analyzed. We had previously identified cooperative developmental functions for *Adamts9* and *Adamts20* in *Adamts9^{+/-};bt/bt* mice, which have more extensive white spotting (Silver et al., 2008) as well as cleft palate, a phenotype absent in mice with either mutation alone (H. Enomoto, C. Nelson, and S.S.A., unpublished data). *Adamts5^{-/-}*; *Adamts9^{+/-}* mice had a considerably higher penetrance of syndactyly (87%) than either *Adamts5^{-/-}* (44%) or *Adamts9^{+/-}* mice, which did not develop syndactyly (Figure 1A). They resembled *Adamts5^{-/-};bt/bt* mice, despite retaining one intact *Adamts9* allele. *Bt/bt*; *Adamts9^{+/-}* mice, which were analyzed at 15.5 days of gestation owing to perinatal lethality from cleft palate, had completely penetrant STS. *Adamts5^{-/-};bt/+*; *Adamts9^{+/-}* mice also had fully penetrant STS (Figure 1A), as well as more affected limbs than *Adamts5^{-/-}*; *Adamts9^{+/-}* or *bt/bt*; *Adamts9^{+/-}* mice (Figure S1). Thus, the allele dosage of these ADAMTS genes is important, and suggests a cooperative mode of action, with ADAMTS5 occupying a key position in IDT regression.

Adamts5, Adamts9, and Adamts20 are Coexpressed in IDT during Web Regression

The temporal restriction of the observed effects of combinatorial *Adamts* allele deletion during IDT regression suggested that these genes were coordinately expressed locally during this process. Accordingly, we determined their mRNA expression patterns during limb development. For *Adamts5*, we previously identified strong perichondrial expression at E14.5 using *in situ* hybridization (McCulloch et al., 2009). β -gal staining was used as a surrogate for *Adamts5* mRNA using an intragenic IRES-lacZ cassette (McCulloch et al., 2009), *in situ* hybridization was utilized for *Adamts20*, and both β -gal staining and *in situ* hybridization were used for *Adamts9*. All aspects of forelimb development anticipate the hindlimb by 0.5–1 day, and similar patterns were seen for each gene in forelimbs and hindlimbs within this chronologic gap. The distal limb lacked significant expression of these *Adamts* genes until E12.5 (*Adamts20*) or E13.5 (*Adamts5*, *Adamts9*). At E11.5, *Adamts5* was expressed in peripheral nerves entering the limb buds, *Adamts9* was expressed in core mesenchyme of the limb-buds, and *Adamts20* was diffusely present in both fore- and hindlimbs (Figures 2A–2C). From E13.5–E15.5, there was strong β -gal staining representing *Adamts5* mRNA in the perichondrium of the digit cartilages and IDT (Figure 2A). *Adamts9* mRNA distribution, identified both by β -gal staining (Figure 2B) and *in situ* hybridization (Figure S3) overlapped considerably with *Adamts5* in the perichondrium of developing digit cartilages and IDT. At E13.5, *Adamts20* expression was seen in IDT and in the medial border of the autopod (Figure 2C).

We also analyzed expression of *Adamts4*, which encodes a potent proteoglycan-degrading enzyme (Arner et al., 1999; Sandy et al., 2001) utilizing an intragenic IRES-lacZ reporter in *Adamts4^{-/-}* mice, which showed very weak staining in the IDT at E13.5 and E14.5 (Figure 2D and data not shown) and undetectable mRNA expression by RT-PCR (Figure 2E). *Adamts4^{-/-}* mice did not develop STS. *Adamts4^{-/-}*; *Adamts5^{-/-}* mice and *Adamts4^{-/-};bt/bt* mice did not have greater penetrance or severity of STS than in the respective single deletions (data not shown). Previous work demonstrated prominent expression of *Adamts1* in IDT from E12.5–E15.5, similar to that described

here for *Adamts5* and *Adamts9* (Thai and Iruela-Arispe, 2002). RT-PCR for the entire subset of proteoglycan-degrading ADAMTS proteases using E13.5 hindlimb autopod RNA (Figure 2E) demonstrated expression of *Adamts15*, but not *Adamts8*, in addition to the genes described above.

IDT in Adamts5^{-/-};bt/bt Autopods Have Reduced Apoptosis

Subsequent mechanistic analysis of STS was undertaken in *Adamts5^{-/-};bt/bt* mice. Since interdigit cells die during digit separation, we evaluated apoptosis in these mice. TUNEL-stained E14.5 *Adamts5^{-/-};bt/bt* hindlimb sections showed reduced apoptosis compared to wild-type controls (Figure 3A). E14.5 autopods were also stained with acridine orange, which identifies apoptotic nuclei (Salas-Vidal et al., 2001), and staining in each interdigital space was scored in a blinded fashion (Figures 3B and 3C). For this analysis, we used littermate *Adamts5^{-/-};bt/+* embryos as controls, since STS is markedly reduced by the presence of a wild-type (*wt*) *Adamts20* allele (Figure 1A). Stained nuclei were less abundant in the *Adamts5^{-/-};bt/bt* limbs, with decreased staining being most evident in IDT between digits 2 and 3 and between digits 3 and 4 of the hindlimbs (Figure 3C), consistent with the highest severity in these webs (Figures S2A and S2B).

The Bmp-Fgf Axis Is Unaffected in Adamts5^{-/-};bt/bt Autopods

BMPs are key mediators of IDT apoptosis and Gremlin antagonizes BMP signaling during IDT resorption (Bandyopadhyay et al., 2006; Guha et al., 2002; Merino et al., 1999a; Weatherbee et al., 2006). *Bmp2*, *Bmp4*, *Bmp7*, and *Gremlin* expression were localized to the IDT, consistent with their role in local signaling, but their expression pattern was essentially similar in *Adamts5^{-/-};bt/bt* mice and control autopods (Figure 3D). These data suggest that ADAMTS proteases do not act upstream of *Bmps* or *Gremlin*. Coexpression of Gremlin protein with ADAMTS5 in HEK293F cells showed no cleavage of Gremlin, suggesting that it is not degraded by ADAMTS5 (data not shown). Thus, lack of web resorption in *Adamts5^{-/-};bt/bt* mice could not be explained by defective BMP expression or by altered levels of the major BMP inhibitor, Gremlin, acting in the IDT. Expression of key BMP targets, *Msx1* and *Msx2*, was unaltered (Figure 3D). *Fgf4* and *Fgf8* were strongly expressed in an overlapping pattern with BMP genes although there was no difference between *Adamts5^{-/-};bt/bt* mice and wild-type control autopods (Figure 3D). Intense expression of these FGFs in IDT was unexpected; to our knowledge, their expression has not been previously reported at this gestational age in the limbs and suggests a dramatic shift from the AER to IDT at E13.5. Immunostaining with an antibody that detects pSmad1/5/8 showed positively stained nuclei in the interdigit cells (Figure 3E), and suggested that intracellular BMP signaling was unaffected in *Adamts5^{-/-};bt/bt* mice, consistent with normal *Msx1* and *Msx2* expression (Figure 3D).

Cleavage of Versican Is Reduced in Adamts5^{-/-};bt/bt Autopods

Since web regression requires clearance of ECM as well as cells, we asked whether removal of ECM was affected in

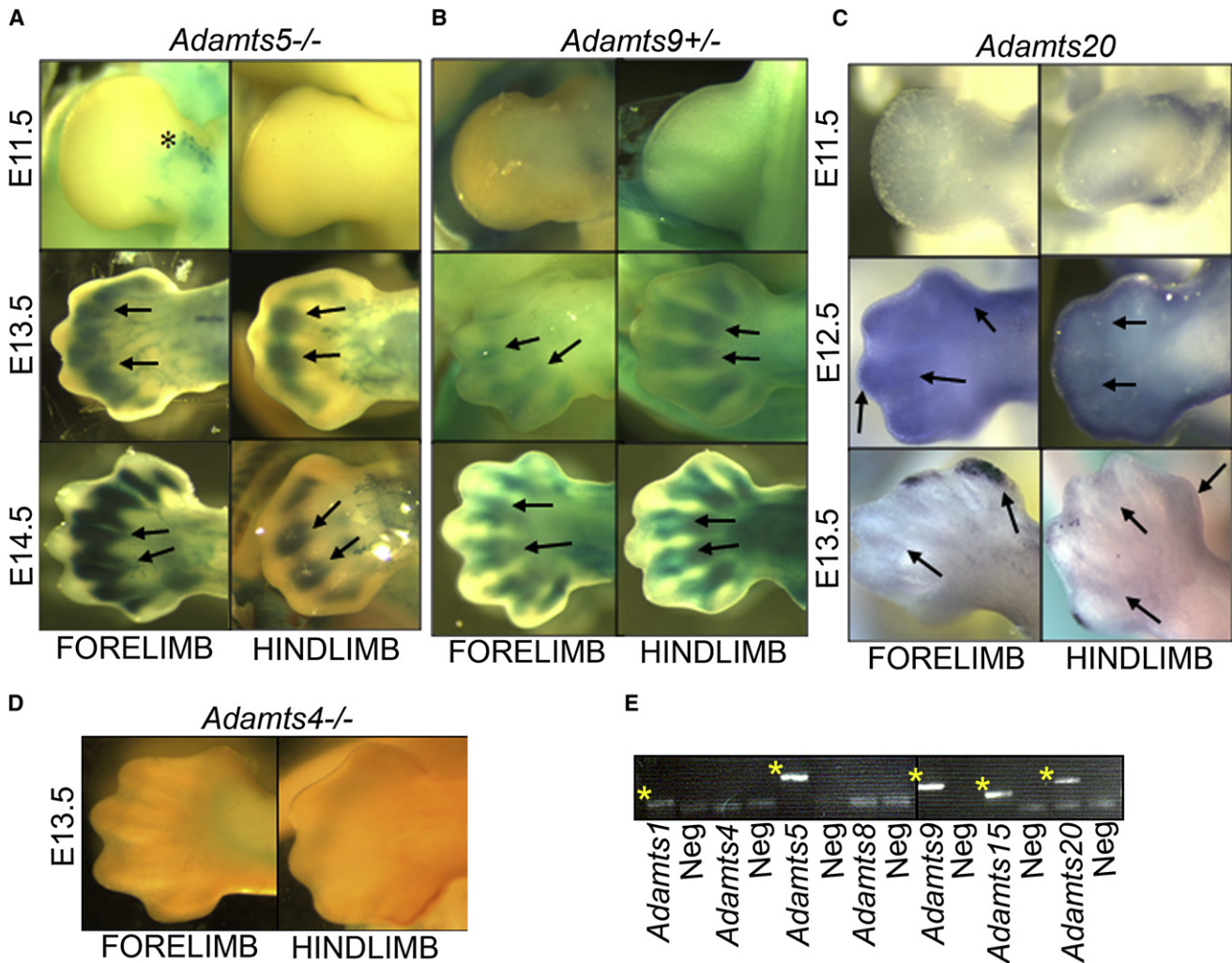


Figure 2. Expression of *Adamts* Genes in the Developing Autopod

(A and B) β -Gal staining (blue-green) was used to profile *Adamts5* (A) and *Adamts9* (B) expression in forelimb and hindlimb autopods from E11.5 through E14.5. Note strong interdigital staining at E13.5 and E14.5 (arrows). The asterisk in the E11.5 *Adamts5*^{-/-} autopod indicates staining of the brachial plexus.

(C) In situ hybridization of *Adamts20* in E11.5, E12.5, and E13.5 autopods. Diffuse expression was seen in the IDT at E12.5 and E13.5, and in the medial and lateral edges of the autopod (arrows).

(D) β -Gal staining of *Adamts4*^{-/-} autopods shows weak expression in forelimb IDT at E13.5.

(E) RT-PCR of RNA extracted from E13.5 wild-type hindlimbs. Specific amplicons are indicated by yellow asterisks. Neg, control PCR using water in place of cDNA.

Adamts5^{-/-}; *bt/bt* mice. Histology of *Adamts5*^{-/-}; *bt/bt* autopods at E16.5, by which time the process of resorption is completed, demonstrated persistence of the IDT with a low cell density and loose, amorphous matrix, suggestive of high proteoglycan content (Figure 4A, left and center panels). Immunohistochemistry demonstrated strong versican staining in this unabsorbed tissue (Figure 4A, right-hand panel). Each of the three relevant ADAMTS proteases, as well as ADAMTS1 and ADAMTS4, can generate a specific C-terminal neopeptide (DPEAAE) upon cleavage of the versican V1 isoform at the Glu-441–Ala-442 peptide bond, that is recognizable either by specific staining on immunohistochemistry, or as a 70 kDa band on western blots (Longpre et al., 2009; Sandy et al., 2001; Silver et al., 2008; Somerville et al., 2003). Anti-DPEAAE

immunohistochemistry showed that cleaved versican was indeed present in the interdigital webs of wild-type mice (Figure 4B, left-hand panel), whereas it was markedly reduced or absent in *Adamts5*^{-/-}; *bt/bt* IDT (Figure 4B, right-hand panel). In contrast, no difference in the distribution of fibronectin, a widely-distributed embryonic ECM component, was observed (data not shown).

Because both reduced versican clearance and reduced apoptosis were present in *Adamts5*^{-/-}; *bt/bt* IDT, we asked whether versican proteolysis was causally involved in regulation of apoptosis via a genetic approach in which we reduced the versican level in *bt* mice. Since lethality of the *Vcan* mutant mouse *hdf* (*heart defect*) (Mjaatvedt et al., 1998) occurs prior to IDT regression, versican cannot be completely deleted in

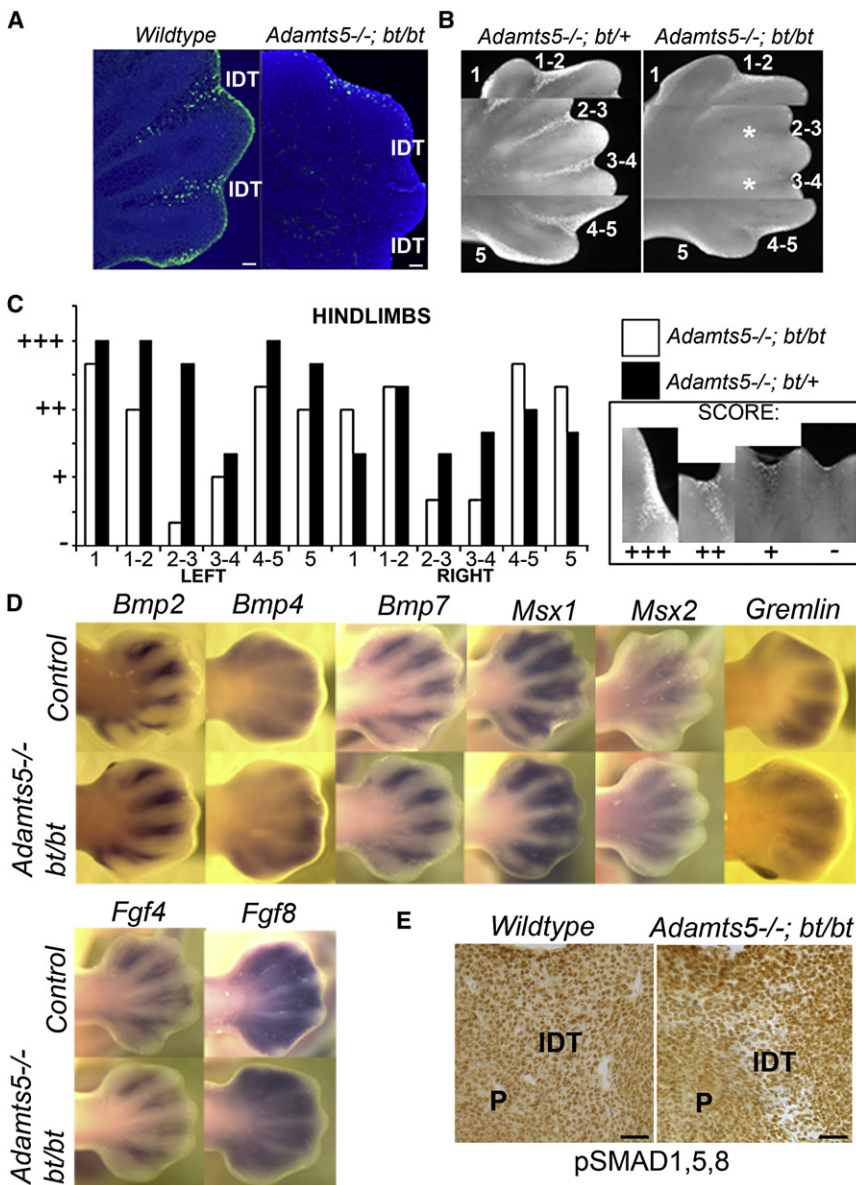


Figure 3. *Adamts5*^{-/-};*bt/bt* Autopods Have Decreased Apoptosis but a Normal BMP-FGF Axis

(A) TUNEL staining of a section from wild-type E14.5 hindlimb autopod (control) shows the expected distribution of apoptotic cells in the IDT (green fluorescence); TUNEL-positive cells are absent in the IDT between digits 2 and 3 as well as between digits 3 and 4 of *Adamts5*^{-/-};*bt/bt* mice. The image is representative of three separately stained hindlimbs. Nuclei are stained blue using DAPI. Scale bar = 50 μ M.

(B) Acridine orange staining of E14.5 hindlimbs showing staining in the IDT of *Adamts5*^{-/-};*bt*^{+/+} mice, whereas staining is absent in the indicated *Adamts5*^{-/-};*bt/bt* IDT (white asterisks). Similar results were obtained in forelimbs of *Adamts5*^{-/-};*bt/bt* mice at E13.5.

(C) Acridine orange staining was scored in each hindlimb interdigital space in a blinded fashion according to the scoring scheme shown on the right. In *Adamts5*^{-/-};*bt/bt* hindlimbs (n = 6), the IDT between hindlimb digits 2 and 3 and digits 3 and 4 consistently had fewer stained cells than the control genotype (*Adamts5*^{-/-};*bt*^{+/+}) hindlimbs (n = 6).

(D) Hindlimb autopods stained by whole mount in situ hybridization with the indicated probes shows comparable mRNA expression in E13.5 *Adamts5*^{-/-};*bt/bt* mice and controls. Similar expression was obtained in forelimbs.

(E) pSmad 1/5/8 immunohistochemistry demonstrates nuclear pSmad staining in both mutant and wild-type E14.5 hindlimb webs. Scale bar = 50 μ M.

Adamts-deficient mice. Therefore, we introduced *Vcan* haploinsufficiency in *bt* mice i.e., we asked if a reduced versican burden could be effectively cleared, and apoptosis could be restored despite the reduced overall level of versican-degrading activity resulting from the absence of ADAMTS20. Unexpectedly, *bt/bt*; *hdf1*^{+/+} mice had 100% penetrance of syndactyly, similar to *Adamts5*^{-/-};*bt/bt* mice, and considerably greater than that observed in either *bt/bt* or *Adamts5*^{-/-} mice (Figure 4C, Figure S4). This genetic interaction suggested that versican cleavage by ADAMTS proteases, and the presence of cleaved versican was required for regression of the IDT.

Fibulin-1, a Cofactor for ADAMTS5-Mediated Versican Proteolysis, Colocalizes with Versican and Influences IDT Regression

Fibulin-1, a modular ECM protein interacting with the G3 domain of versican, was previously reported to be a cofactor for

immunofluorescence in E14.5 *wt* and *Adamts5*^{-/-};*bt/bt* hindlimbs. Fibulin-1 colocalized with versican in the perichondrium in both genotypes (Figure 5A shows wild-type staining). ADAMTS5 is the most active versicanase among the three proteases and is most closely related to ADAMTS1. Because the highest penetrance of STS among single gene deletions was in *Adamts5*^{-/-} mice, we used a cell-based assay to determine whether fibulin-1 influenced ADAMTS5 processing of versican. ADAMTS5 was expressed alone or was coexpressed with fibulin-1 isoforms with different C-terminal domains, fibulin-1C and -1D, followed by incubation of the conditioned medium from these cells with versican-rich medium from vascular smooth muscle cells. Cotransfection of ADAMTS5 with fibulin-1C or -1D led to a significant increase in versicanase activity, as indicated by increased levels of the 70 kDa versican cleavage fragment containing the DPEAAE neopeptide on western blots (Figures 5B and 5C). Fibulin-1 was not proteolytically modified by ADAMTS5.

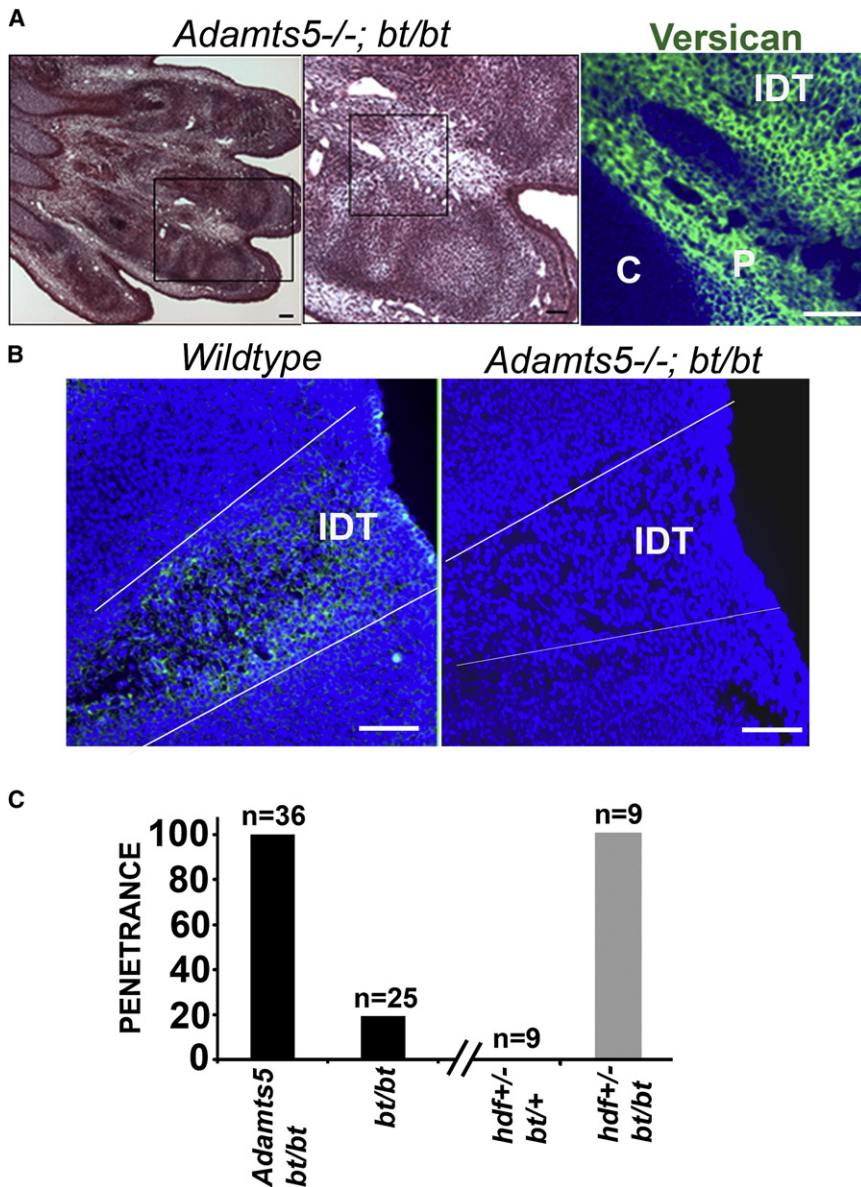


Figure 4. Reduced Versican Processing in *Adamts5*^{-/-}; *bt/bt* IDT, and Increased STS in *bt/bt*; *Vcan*^{+/-} mice

(A) An E16.5 hindlimb from an *Adamts5*^{-/-}; *bt/bt* mouse shows lack of IDT resorption between digits 3 and 4 (boxed area, left-hand panel). The boxed area is enlarged in the center panel to illustrate a low cell density and loose ECM in the unresorbed IDT, suggestive of proteoglycan accumulation. The nonregressed ECM stains strongly with an anti-versican GAG β antibody (right-hand panel, green signal). Scale bar = 50 μ m.

(B) Cleaved versican identified by anti-DPEAAE staining (green) is present in the IDT of an E14.5 wild-type hindlimb (left-hand panel). In contrast, greatly reduced anti-DPEAAE staining is seen in E14.5 *Adamts5*^{-/-}; *bt/bt* hindlimb IDT (right-hand panel). Scale bar = 50 μ m.

(C) STS in *bt/bt*; *hdf*^{+/+} mice. Data indicating penetrance in *Adamts5*^{-/-}; *bt/bt* mice, and *bt/bt* mice (black bars), are taken from Figure 1. Note the lack of syndactyly in compound heterozygotes of *bt* and *hdf* and the greatly increased penetrance in *bt/bt*; *hdf*^{+/-} mice (gray bar).

Versican Expression and Proteolysis Are Spatially Regulated during IDT Regression

Versican is a widely distributed proteoglycan in embryonic ECM, and a substrate of *Adamts5* (Longpre et al., 2009), *Adamts9* (Somerville et al., 2003), and *Adamts20* (Silver et al., 2008). Since versican proteolysis was defined as a critical event in web regression, we determined *Vcan* expression and localization relative to ADAMTS5 and fibulin-1 in further detail using in situ hybridization and immunolocalization. During limb development, *Vcan* was strongly upregulated in the precartilaginous mesenchyme of prospective digit cartilages at E12.5, whereas after E13.5, *Vcan* mRNA was confined to the perichondrium of

both forelimbs and hindlimbs and to the tips of the digits (Figure 6A). At E12.5 and E13.5, some *Vcan* expression was also present in IDT (Figure 6A). Thus, its expression overlapped with *Adamts5*, *Adamts9*, and *Adamts20* during autopod morphogenesis and web regression and corresponded temporally with them. To precisely define their spatial relationships, we used immunofluorescence to detect versican, cleaved versican, fibulin-1, and ADAMTS5 in serial sections of E14 hindlimb autopods. Versican localized to the broadest tissue domain, extending from the edge of digit cartilage to the IDT, where substantially lower staining intensity than perichondrium was seen (Figure 6B). Fibulin-1 overlapped with versican in the perichondrium, and ADAMTS5 was juxtaposed with the most peripheral region of versican and fibulin-1 staining. Intriguingly, cleaved versican (representing cleaved N-terminal fragments ending in Glu-441) was located primarily in the IDT (Figure 6B).

Given this observed effect and colocalization of fibulin-1 with versican, we hypothesized that fibulin-1 enhanced ADAMTS activity during IDT regression, and assessed the penetrance and severity of STS in *bt/bt*; *Fbln1*^{+/-} mice. *Fbln1*^{-/-} mice have severe vascular and lung anomalies and die perinatally (Cooley et al., 2008; Kostka et al., 2001), and thus *bt/bt*; *Fbln1*^{-/-} mice were not generated. *bt/bt*; *Fbln1*^{+/-} mice developed STS with high penetrance, similar to *Adamts5*^{-/-}; *bt/bt* mice (Figure 5D, Figure S4). This finding strongly suggested that fibulin-1 acted as a cofactor for at least one ADAMTS in IDT regression. We conclude that in the absence of *Adamts20* (*bt/bt* genotype), *Fbln1* haploinsufficiency lowered the activity of ADAMTS5 similar to that resulting from deficiency of both *Adamts20* and *Adamts5* and also possibly reduced the activity of one or more other ADAMTS proteases.

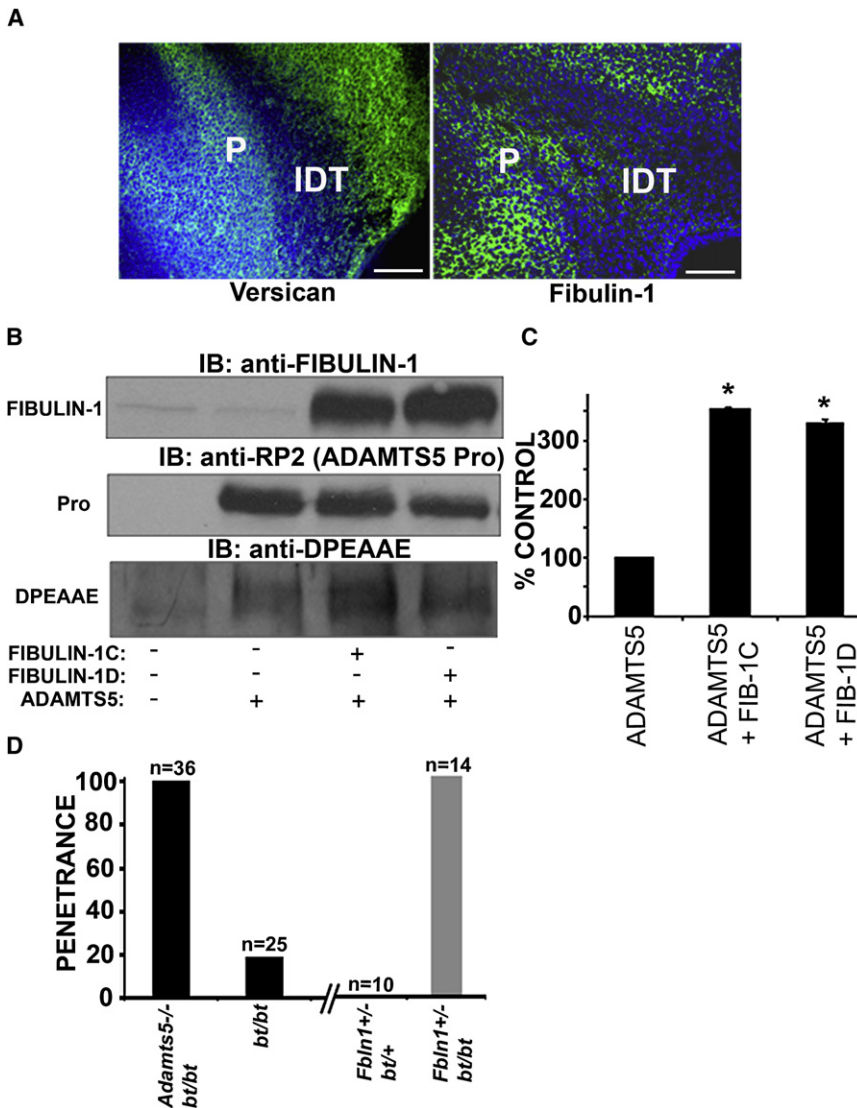


Figure 5. Fibulin-1 and Versican Colocalize in the IDT and Fibulin-1 Acts as a Cofactor for *Adamts5*-Mediated Versican Proteolysis

(A) Intact versican (GAGB, green, left-hand panel) has a similar localization as fibulin-1 (green, right-hand panel) in E14.5 wild-type hindlimb perichondrium (P). A weak signal is present in IDT. These data are representative of three stained autopods. Nuclei are stained blue by DAPI. Scale bar = 50 μ M.

(B) Fibulin-1 enhances ADAMTS5 processing of versican. Western blots show expression of fibulin-1C, and fibulin-1D (upper panel) in cell lysates from HEK293F cells cotransfected with full-length *Adamts5* (detected by a propeptide specific antibody RP-2, center panel). Anti-DPEAAE was used to detect the cleaved 70 kDa versican species in the medium (lower panel).

(C) Quantification of anti-DPEAAE reactive molecular species in medium of cells expressing ADAMTS5 alone, or ADAMTS5 plus fibulin-1C or fibulin 1-D. Levels of anti-DPEAAE-reactive peptide obtained by densitometry were normalized to levels of *Adamts5* propeptide and are representative of four independent experiments (data show mean \pm SEM). There is a statistically significant enhancement of versican processing by ADAMTS5 in the presence of both fibulin-1 isoforms (Student's t test, * $p < 0.05$).

(D) Penetrance of syndactyly is increased in *bt/bt*; *Fbln1*^{+/-}/*bt*⁺ mice compared to *bt/bt* and *Fbln1*^{+/-}/*bt*⁺ mice, suggesting a genetic interaction between *Adamts5* and *Fbln1* (Note: *Fbln1* haploinsufficiency leads to STS in mice lacking ADAMTS20, thus uncovering a functional association with another ADAMTS protease, most likely ADAMTS5, as evidenced by findings in [B]). Data for penetrance in *Adamts5*^{-/-}/*bt/bt* mice and *bt/bt* mice (black bars) are taken from Figure 1.

These data suggest that only the most peripherally located versican in the digit perichondrium is likely to be cleaved by ADAMTS5, and demonstrate that cleaved versican is localized with the cell population that is destined to undergo apoptosis.

Application of Ectopic BMP4 Rescues Apoptosis in *Adamts5*^{-/-}/*bt/bt* IDT Without Inducing Versican Cleavage

We tested whether IDT cells in *Adamts5*^{-/-}/*bt/bt* hindlimbs were responsive to BMP induction of apoptosis by local application of exogenous BMP4. Recombinant active BMP4, TGF β 2, or bovine serum albumin (BSA, negative control) in a microbead carrier was delivered to the IDT between digits 3 and 4 of the right hindlimbs of E13.75 *Adamts5*^{-/-}/*bt/bt* autopods, since this interdigital space consistently presented the most severe syndactyly (Figure 3C, Figures S2A and S2B). Local application of BMP4 but not BSA induced apoptosis in the IDT (Figure 6C), yet did so in the absence of increased versican cleavage in the vicinity of the bead. Although mice lacking both TGF β 2 and TGF β 3

have STS (Dunker et al., 2002), a bead soaked in TGF β 2 did not induce apoptosis in these autopods (data not shown). These data suggest that in the presence of sufficiently high BMP levels, apoptosis can be induced without concomitant versican processing. These data also suggest that ADAMTS proteases are not downstream effectors of BMPs during IDT apoptosis.

Application of Cleaved Versican Induces Apoptosis in *Adamts5*^{-/-}/*bt/bt* Webs

Since the genetic interactions described above, together with the presence of cleaved versican in the interdigital webs pointed to a potential mechanistic role for cleaved versican, we generated recombinant G1-DPEAAE⁴⁴¹ versican representing a product of ADAMTS activity (Figure 7A). A bead soaked in conditioned medium from HEK293F cells stably expressing this fragment was inserted into the mutant webs as described above for BMP-4. Medium from cells transfected with an empty vector was used as the negative control. As shown in Figure 7B, the versican fragment induced apoptosis in *Adamts5*^{-/-}/*bt/bt*

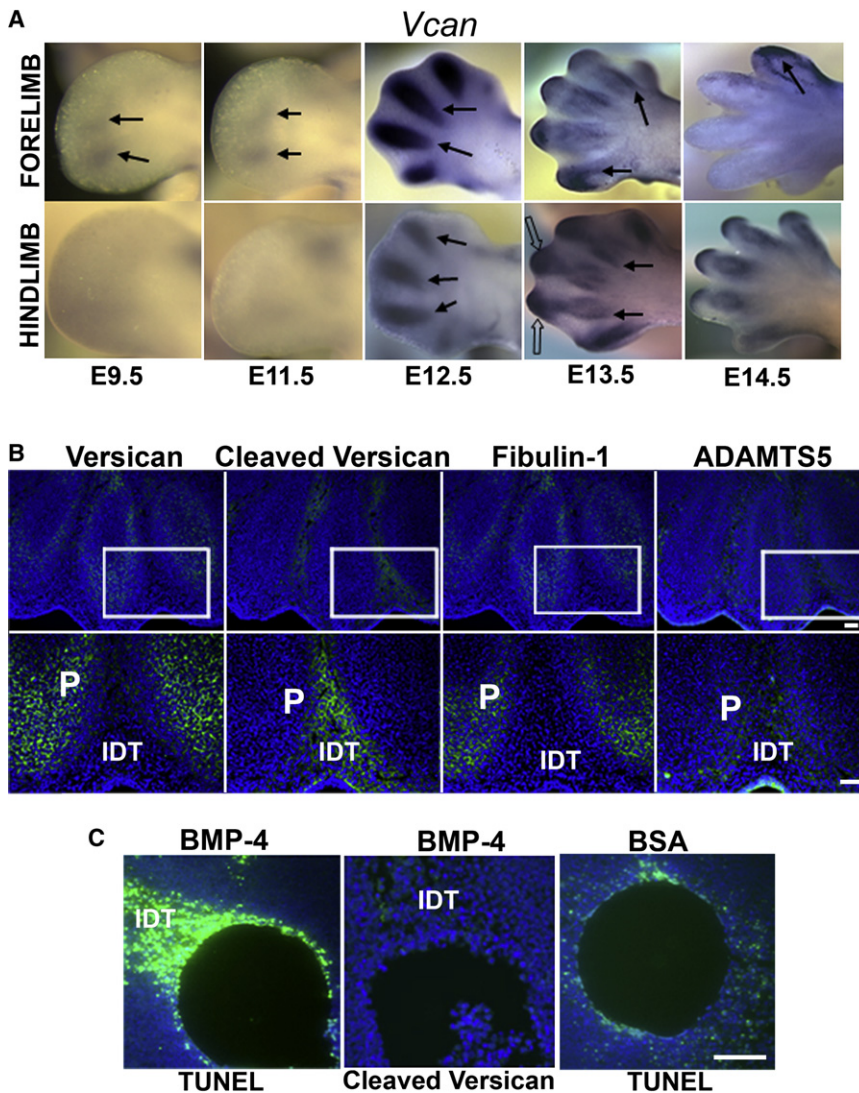


Figure 6. Versican Expression and Localization during Autopod Development and the Effect of Local BMP4 Application on Apoptosis and Versican Proteolysis

(A) Whole-mount ISH with a *Vcan* probe shows strong expression in the precartilaginous mesenchyme of digital rays at E12.5 (arrows), with forelimb expression anticipating the hindlimb. At later stages, *Vcan* is strongly expressed in perichondrium (arrows at E13.5), with weak expression in the IDT.

(B) Serial sections from a wild-type E14.0 hindlimb autopod were immunostained with indicated antibodies to show the precise relationship between versican, cleaved versican, fibulin-1, and ADAMTS5. The boxed regions in the upper panels are enlarged in the lower panels. Cleaved versican is located in the IDT whereas the strongest signals for intact versican and fibulin-1 are present in the perichondrium (P). ADAMTS5 is located at the boundary between perichondrium and IDT.

(C) Implantation of a BMP4-soaked bead in E13.75 *Adams5*^{-/-};*bt/bt* hindlimb IDT leads to apoptosis (TUNEL) but not to versican cleavage, whereas a bead soaked in BSA did not induce cell death. The result is representative of three independent experiments.

The observed effects of allele dosage suggest that the combined proteolytic activity of at least three ADAMTS proteases, ADAMTS5, ADAMTS9, and ADAMTS20 (and possibly ADAMTS1) normally maintains proteolysis of versican above a critical hypothetical threshold required for complete IDT regression (Figure 7D). Removal of a single versican-degrading ADAMTS protease may reduce proteolytic activity to around the level of the threshold, in which

webs ($n = 6$), whereas in the control experiments ($n = 6$) apoptosis was primarily seen at the margins of the bead. These data suggest that the product of versican cleavage by ADAMTS proteases enabled interdigital apoptosis.

DISCUSSION

This work identifies a mechanism for ECM clearance during web regression and suggests that distinct *Adams* gene products work cooperatively with each other and synchronously with proapoptotic mechanisms during web regression. The temporal and spatial overlap between ADAMTS proteases and versican, together with persistent uncleaved versican and decreased DPEAAE immunoreactivity in *Adams5*^{-/-};*bt/bt* IDT, are strongly suggestive of an essential role for ADAMTS5, ADAMTS9, and ADAMTS20 in versican processing during IDT regression. The data not only suggest that ADAMTS proteolysis of versican during IDT resorption is facilitated by fibulin-1, but also that cleaved versican is required for web regression, possibly by sensitization of IDT cells to proapoptotic factors such as BMPs (Figure 7C).

case incompletely penetrant syndactyly is observed, as in *bt/bt* or *Adams5*^{-/-} mice (Figure 7D). When two or more ADAMTS proteases are deleted (e.g., *Adams5*^{-/-};*bt/bt* mice), proteolytic activity drops below the threshold and a higher penetrance of syndactyly is observed (Figure 7D). Subthreshold proteolysis also results from reduction of fibulin-1, a cofactor for ADAMTS5, and therefore has a similar outcome as reduction of *Adams5* alleles in *bt* mice (Figure 7D). Fibulin-1 may also act as a cofactor for other ADAMTS proteases. Alternately, *Fbln1* haploinsufficiency may affect the formation of versican-containing networks. A complex synpolydactyly has been reported as a result of rearrangement of *FBLN1* in humans (Debeer et al., 2002). However, limb defects have not been reported in *Fbln1*^{-/-} mice.

The observed variation in severity of STS, and the fact that not all interdigital spaces are affected in compound ADAMTS-deficient mice, strongly suggests that additional versican-degrading ADAMTS proteases are involved. We excluded a role for ADAMTS4 by genetic analysis and showed that *Adams4* was not expressed in the autopod, but our studies most likely underestimated the contribution of ADAMTS9, since it cannot be

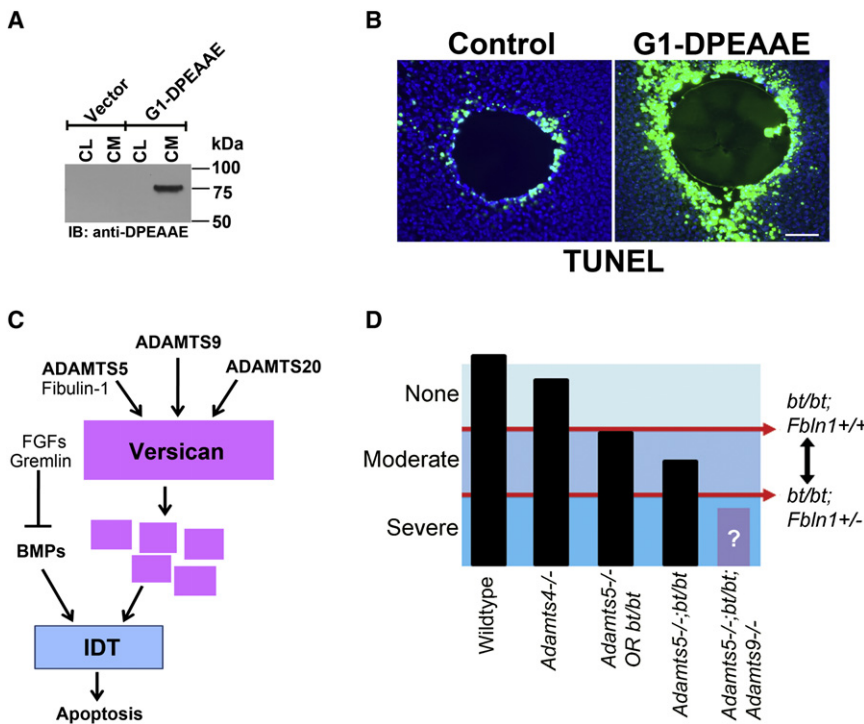


Figure 7. Versican G1-DPEAAE⁴⁴¹ Fragment Induces Apoptosis

(A) Western blotting shows production and secretion of the G1-DPEAAE⁴⁴¹ fragment in conditioned medium (CM) of stably transfected cells. The absence of immunoreactivity in cell lysate (CL) may reflect the relative abundance of accumulated G1-DPEAAE⁴⁴¹ fragment in CM.

(B) A bead soaked in G1-DPEAAE⁴⁴¹ fragment induced greater apoptosis over a wider distance compared to the control bead. The result is representative of six independent experiments for both the G1-DPEAAE⁴⁴¹ fragment and control media.

(C) A proposed model for the role of ADAMTS proteases and versican in IDT regression, suggesting that ADAMTS-generated versican fragments may work synchronously with BMPs and create a permissive environment for BMP induction of apoptosis.

(D) Cooperative model of ADAMTS action. Cooperative maintenance of the required threshold of versican proteolysis is provided by spatial and temporal overlap of versican-degrading ADAMTS proteases in the IDT. Because two additional versican-degrading proteases (*Adamts1* and *Adamts9*) are implicated, we speculate on the existence of a second threshold below which more severe syndactyly, or STS affecting all web spaces, may be seen (gray bar). Alteration of the level of fibulin-1 alters the proteolytic threshold by reducing ADAMTS5 activity.

completely deleted in IDT at the present time. *Adamts1* is highly expressed in the IDT during web regression (Thai and Iruela-Arispe, 2002) but combinatorial deletion of *Adamts1* and *Adamts5* is currently untenable since these genes are tightly linked (70 kb apart) on mouse chromosome 16 (Koo et al., 2007).

Taken together, the experimental observations comprising genetic interactions, overlapping mRNA expression and protein localization, and biochemical interactions, are consistent with the existence of a molecular network in ECM comprised of ADAMTS5, ADAMTS9, ADAMTS20, versican, and fibulin-1, that influences apoptosis during IDT resorption. Binary biochemical interactions have been previously demonstrated between versican and fibulin-1, ADAMTS1 and fibulin-1, and ADAMTS proteases (specifically, ADAMTS1, ADAMTS4, ADAMTS5, ADAMTS9, and ADAMTS20) and versican (Aspberg et al., 1999; Lee et al., 2005; Longpre et al., 2009; Olin et al., 2001; Sandy et al., 2001; Silver et al., 2008; Somerville et al., 2003).

We investigated possible connections between this extracellular network and apoptosis in vivo. The data suggest that ADAMTS proteases are not upstream of either BMP- or FGF-signaling mechanisms, since the BMP-FGF axis and BMP signaling were unimpaired in the absence of ADAMTS5 and ADAMTS20. Induction of apoptosis by BMP4 without concurrent versican proteolysis in *Adamts5^{-/-};bt/bt* IDT suggests that: (1) in the presence of a high local concentration of BMP, versican proteolysis was not required, and (2) neither ADAMTS5 nor ADAMTS20 normally acted immediately downstream of BMP4. Normal BMP and FGF expression and BMP signaling in *Adamts5^{-/-};bt/bt* autopods argues against a role for ADAMTS proteases in release of BMPs or FGFs sequestered in ECM. It

has been established that BMPs induce apoptosis when the local environment is permissive (Ganan et al., 1996; Guha et al., 2002; Merino et al., 1999b; Zou and Niswander, 1996) and we considered whether ADAMTS proteolysis of versican contributed to the permissiveness of the cellular environment at the critical developmental stage when IDT regression occurs.

Initially, we asked whether versican was simply a passive target of the ADAMTS proteases to be cleared concurrently with cells as part of normal IDT regression. However, since *hdf^{+/-}* mice do not have STS, and because STS in *bt/bt; hdf^{+/-}* mice is as penetrant as in *bt/bt; Adamts5^{-/-}* mice, we propose that cleaved rather than intact versican is necessary for web regression. The observation of cleaved versican within the IDT at a site remote from the highest concentrations of intact versican raises the intriguing possibility that versican fragments may move into the IDT where they may bind to cells or disrupt cell-matrix interactions. The traditional developmental roles of versican as an antiadhesive molecule, a barrier for cell migration, or in defining migratory pathways of neural crest cells (Dutt et al., 2006; Perissinotto et al., 2000) implied passive mechanisms. However, recent work has demonstrated intriguing effects of versican and recombinant versican domains on cell proliferation, senescence, and apoptosis, although these are poorly understood (LaPierre et al., 2007; Suwan et al., 2009). Since the requirement for versican processing is bypassed by insertion of a BMP4 soaked bead, we speculated that versican fragments may lower the threshold of BMP required to induce apoptosis. Indeed, the versican G1-DPEAAE⁴⁴¹ fragment, expressed as a recombinant protein, could induce apoptosis in the mutant web. We propose that proteolysis of versican is permissive for

BMP-induced apoptosis during normal development, i.e., concurrent versican processing and BMP upregulation enable interdigit cell apoptosis (Figure 7C).

The evolution of mammalian limb development to require multiple proteases for web regression is, upon initial contemplation, quite surprising, since nature is parsimonious. However, *Adamts5*, *Adamts1*, *Adamts9*, and *Adamts20* mRNAs are also expressed in an overlapping fashion at other sites during development (Jungers et al., 2005; McCulloch et al., 2009; Thai and Iruela-Arispe, 2002). Versican, fibulins, and these versican-degrading ADAMTS proteases are all present in the developing cardiac outflow tract, during craniofacial development, and in the arterial wall, myocardium, skin, and central nervous system (Bode-Lesniewska et al., 1996; Kern et al., 2007; Stankunas et al., 2008; Zhang et al., 1995, 1996). Recent work implicated versican processing by ADAMTS1 in remodeling of the embryonic myocardium and cardiac outflow tract (Kern et al., 2007; Stankunas et al., 2008) and during ovulation (Russell et al., 2003). It is possible, although as yet unconfirmed, that the molecular network identified here, as well as bioactive versican fragments, may participate in other developmental processes as well.

ADAMTS5 is a key pathogenic protease and drug target in arthritis, since *Adamts5*^{-/-} mice do not develop arthritis following induction of inflammation or mechanical instability in their knees (Glasson et al., 2005; Stanton et al., 2005). ADAMTS5 was previously thought not to have a developmental role. The proposed threshold model of ADAMTS proteolysis (Figure 7A) suggests that the detection of *Adamts* phenotypes may be masked in mice lacking a single ADAMTS protease, or that the severity of observed phenotypes may be underestimated. Combinatorial transgenes for proteoglycan-degrading ADAMTS proteases are therefore likely to be insightful and relevant to several morphogenetic processes.

EXPERIMENTAL PROCEDURES

Additional methods and/or details are provided in the Supplemental Experimental Procedures.

Analysis of Transgenic Mice—Mouse Strains, Embryo Preparation, and β -Gal Histochemistry

All animal procedures were done at the Cleveland Clinic under an Institutional Animal Care and Use Committee approved protocol. Mice with targeted inactivation of *Adamts5* (6.129P2-*Adamts5*^{tm1DgeniJ}, referred to as *Adamts5*^{-/-}) (McCulloch et al., 2009), *Adamts4*, and *Adamts9*, were generated by Deltagen (San Mateo, CA) and purchased from Jackson Laboratories (Bar Harbor, ME), *Adamts4* and *Adamts9*) or Deltagen (*Adamts9*). A mutant *Adamts20* allele, *beltd*, (*Adamts20*^{bt-Bel1} referred to as *bt*) (Rao et al., 2003) a *Vcan* mutant allele (*heart defect*, *hdf*) (Mjaatvedt et al., 1998), and *Fbln1*-deficient mice (Cooley et al., 2008) were previously described. All observations were made in alleles that were backcrossed extensively to C57Bl/6 (*Adamts5*, eight generations; *Adamts9* and *bt*, ten generations each; *Fbln1*, seven generations; *hdf*, ten generations). These genes are expected to segregate independently, so combinatorial transgenic mice were generated by interbreeding. STS was scored as described in the Supplemental Experimental Procedures.

Microcomputerized Tomography (mCT) Analysis

The following genotypes (no. of mice) were examined *Adamts5*^{-/-}, *bt/bt* mice (16); *Adamts5*^{+/+}, *+/bt* (1); *Adamts5*^{+/+}, *bt/bt* (1); *Adamts5*^{+/-}, *+/bt* (1); *Adamts5*^{-/-}, *+/bt* (2); *Adamts5*^{+/-} (1); wild-type (1). Mouse limbs were fixed in 70% ethanol and scanned on an eXplore Locus SP instrument (General

Electric). The scans were done at 80 kV peak and 500 μ A with an exposure time of 3000 ms. Three hundred and sixty views were done in a 1° increment over 360°. Scans were reconstructed using GE reconstruction software yielding a postreconstruction resolution of 26 microns. Scans were visualized using GE Health Care Micro-View version ABA 2.1.2.

β -Gal Histochemistry, In Situ Hybridization, IHC, and RT-PCR

Timed gestations, tissue fixation, and β -gal histochemistry are described in the Supplemental Experimental Procedures. Digoxigenin-labeled cRNA probes were generated using reagents from Roche. Embryos obtained from timed gestations were processed for in situ hybridization (ISH) as described in the Supplemental Experimental Procedures. Antibodies and methods used for IHC, RT-PCR primers, and reaction conditions are described in the Supplemental Experimental Procedures.

Detection of Apoptosis Using Acridine Orange Staining and TUNEL Assays

E14.5 embryo limbs were incubated in PBS for 30 min at room temperature and in 0.1 μ g/ml acridine orange (AO) (Sigma-Aldrich) in PBS for 10 min. Limbs were washed twice in PBS and viewed under an inverted fluorescent microscope (Leica) within 2 hr of staining. *Adamts5*^{-/-}; *bt/bt* and *Adamts5*^{-/-}; *bt*⁺ littermates (controls) were stained with AO. Apoptosis was scored by one of the authors (L.J.D.) blinded to the genotype. Detection of apoptotic cells by the TUNEL method was done using a kit (Promega Corp, Madison, WI).

Ex Vivo Limb Culture and Bead Application

Affigel beads (Bio-Rad, Hercules, CA) were soaked in 100 μ g/ml recombinant BMP-4 (R&D systems, Minneapolis, MN), 50 μ g/ml recombinant TGF β , 100 μ g/ml Bovine Serum Albumin (BSA) (Sigma-Aldrich), conditioned medium of G1-DPEAAE⁴⁴¹ expressing HEK293F cells, or the control medium for 1 hr at room temperature. E13.75 *Adamts5*^{-/-}; *bt/bt* hindlimb autopods were dissected and placed in culture medium optimized for these cultures (1:1 DMEM:Ham's F12 plus 0.1% FBS). Size-matched presoaked Affigel beads were inserted in the web space between digits 3 and 4. Autopods were placed on a Nuclepore 8 μ m pore-size filter (Whatman, Florham Park, NJ) in a 24-well tissue culture dish, and cultured at the air-liquid interface. Hindlimbs were incubated for 14 hr at 37°C in 5% CO₂ followed by AO staining or TUNEL assay on paraffin sections. For bead insertion of G1-DPEAAE⁴⁴¹, Nuclepore 0.1 μ m pore size track-etch membrane was used.

Cell Culture, Transfections, Versicanase Assay, and Western Blotting

HEK293F cells (ATCC, Manassus, VA) were cultured in Dulbecco's Modified Eagles Medium (DMEM) supplemented with 10% FBS and antibiotics. Expression plasmids for Myc-tagged *Adamts5*, fibulin-1C and -1D, and Gremlin, were transiently cotransfected into HEK293F cells using FUGENE-6 (Roche Diagnostics, Indianapolis, IN). In the case of control *Adamts5* cotransfection, empty vector (pcDNA3.1 MycHis, Invitrogen) was cotransfected with the *Adamts5* construct. Serum-free media and cell lysates were collected after 24 hr. Cells were lysed in 1% Triton X-100, 10 mM Tris HCl (pH 7.6) containing complete protease inhibitor cocktail (Roche Diagnostics, Indianapolis, IN). Conditioned medium was combined with versican-rich medium obtained from cultured human vascular smooth muscle cells at a 1:1 ratio, and incubated for 12–18 hr at 37°C, followed by treatment with protease-free chondroitinase ABC (Seikagaku, Tokyo, Japan) for 2 hr at 37°C. Western blotting was done under reducing conditions using anti-DPEAAE (Affinity Bioreagents, Golden, CO), anti-fibulin-1 (Sasaki et al., 1995), or anti-myc monoclonal antibody 9E10 (Invitrogen, Carlsbad, CA) and enhanced chemiluminescence (ECL, GE Healthcare, Piscataway, NJ). Band intensity was quantitated using IMAGE J software (NIH, Bethesda, MD). A type 1 (paired), 2-tailed Student's *t* test was used to determine whether the normalized data obtained from the ImageJ software were statistically significant.

SUPPLEMENTAL DATA

Supplemental Data include four figures and Supplemental Experimental Procedures and are available at [http://www.cell.com/developmental-cell/supplemental/S1534-5807\(09\)00390-6/](http://www.cell.com/developmental-cell/supplemental/S1534-5807(09)00390-6/).

ACKNOWLEDGMENTS

We thank Roche Pharmaceuticals, Corey Mjaatvedt and Christine B. Kern for *hdf* mice, David Beier for *bt* mice, Vernique Lefebvre, Radhika Atit, and Richard Harland for cDNAs, Preston Alexander and John Sandy for ADAMTS5 antibodies, Amanda Allamong and Michael Braun for assistance with histology, and James Lang for photography. Dieter Zimmermann provided the versican expression plasmid. This work was supported by National Institutes of Health grants to S.S.A. (AR49930 and AR53890) and W.S.A. (HL095067), the Arthritis Foundation (Northeast Ohio Chapter Award to S.S.A.) and the American Heart Association (Grant-in-Aid 0755346U to W.S.A.). Histology and mCT was done at the Cleveland Clinic Musculoskeletal Core Center (supported by NIH grant AR050953).

Received: October 2, 2008

Revised: September 10, 2009

Accepted: September 22, 2009

Published: November 16, 2009

REFERENCES

- Apte, S.S. (2009). A disintegrin-like and metalloprotease (reprolysin-type) with thrombospondin type 1 motif (ADAMTS) superfamily-functions and mechanisms. *J. Biol. Chem.*, in press. Published online September 4, 2009. 10.1074/jbc.R109.052340.
- Arner, E.C., Pratta, M.A., Trzaskos, J.M., Decicco, C.P., and Tortorella, M.D. (1999). Generation and characterization of aggrecanase. A soluble, cartilage-derived aggrecan-degrading activity. *J. Biol. Chem.* 274, 6594–6601.
- Aspberg, A., Adam, S., Kostka, G., Timpl, R., and Heinegard, D. (1999). Fibulin-1 is a ligand for the C-type lectin domains of aggrecan and versican. *J. Biol. Chem.* 274, 20444–20449.
- Bandyopadhyay, A., Tsuji, K., Cox, K., Harfe, B.D., Rosen, V., and Tabin, C.J. (2006). Genetic analysis of the roles of BMP2, BMP4, and BMP7 in limb patterning and skeletogenesis. *PLoS Genet.* 2, e216.
- Barth, J.L., Argraves, K.M., Roark, E.F., Little, C.D., and Argraves, W.S. (1998). Identification of chicken and *C. elegans* fibulin-1 homologs and characterization of the *C. elegans* fibulin-1 gene. *Matrix Biol.* 17, 635–646.
- Bode-Lesniewska, B., Dours-Zimmermann, M.T., Odermatt, B.F., Briner, J., Heitz, P.U., and Zimmermann, D.R. (1996). Distribution of the large aggregating proteoglycan versican in adult human tissues. *J. Histochem. Cytochem.* 44, 303–312.
- Boulet, A.M., Moon, A.M., Arenkiel, B.R., and Capecchi, M.R. (2004). The roles of Fgf4 and Fgf8 in limb bud initiation and outgrowth. *Dev. Biol.* 273, 361–372.
- Cooley, M.A., Kern, C.B., Fresco, V.M., Wessels, A., Thompson, R.P., McQuinn, T.C., Twal, W.O., Mjaatvedt, C.H., Drake, C.J., and Argraves, W.S. (2008). Fibulin-1 is required for morphogenesis of neural crest-derived structures. *Dev. Biol.* 319, 336–345.
- Dahn, R.D., and Fallon, J.F. (2000). Interdigital regulation of digit identity and homeotic transformation by modulated BMP signaling. *Science* 289, 438–441.
- Debeer, P., Schoenmakers, E.F., Twal, W.O., Argraves, W.S., De Smet, L., Fryns, J.P., and Van De Ven, W.J. (2002). The fibulin-1 gene (FBLN1) is disrupted in a t(12;22) associated with a complex type of synpolydactyly. *J. Med. Genet.* 39, 98–104.
- Dunker, N., Schmitt, K., and Kriegelstein, K. (2002). TGF- β is required for programmed cell death in interdigital webs of the developing mouse limb. *Mech. Dev.* 113, 111–120.
- Dutt, S., Kleber, M., Matasci, M., Sommer, L., and Zimmermann, D.R. (2006). Versican V0 and V1 guide migratory neural crest cells. *J. Biol. Chem.* 281, 12123–12131.
- Ganan, Y., Macias, D., Duterque-Coquillaud, M., Ros, M.A., and Hurler, J.M. (1996). Role of TGF β s and BMPs as signals controlling the position of the digits and the areas of interdigital cell death in the developing chick limb autopod. *Development* 122, 2349–2357.
- Glasson, S.S., Askew, R., Sheppard, B., Carito, B., Blanchet, T., Ma, H.L., Flannery, C.R., Peluso, D., Kanki, K., Yang, Z., et al. (2005). Deletion of active ADAMTS5 prevents cartilage degradation in a murine model of osteoarthritis. *Nature* 434, 644–648.
- Gross, J., and Lapiere, C.M. (1962). Collagenolytic activity in amphibian tissues: a tissue culture assay. *Proc. Natl. Acad. Sci. USA* 48, 1014–1022.
- Guha, U., Gomes, W.A., Kobayashi, T., Pestell, R.G., and Kessler, J.A. (2002). In vivo evidence that BMP signaling is necessary for apoptosis in the mouse limb. *Dev. Biol.* 249, 108–120.
- Hesselton, D., Newman, C., Kim, K.W., and Kimble, J. (2004). GON-1 and fibulin have antagonistic roles in control of organ shape. *Curr. Biol.* 14, 2005–2010.
- Jungers, K.A., Le Goff, C., Somerville, R.P., and Apte, S.S. (2005). Adamts9 is widely expressed during mouse embryo development. *Gene Expr. Patterns* 5, 609–617.
- Kern, C.B., Norris, R.A., Thompson, R.P., Argraves, W.S., Fairey, S.E., Reyes, L., Hoffman, S., Markwald, R.R., and Mjaatvedt, C.H. (2007). Versican proteolysis mediates myocardial regression during outflow tract development. *Dev. Dyn.* 236, 671–683.
- Kimata, K., Oike, Y., Tani, K., Shinomura, T., Yamagata, M., Uritani, M., and Suzuki, S. (1986). A large chondroitin sulfate proteoglycan (PG-M) synthesized before chondrogenesis in the limb bud of chick embryo. *J. Biol. Chem.* 261, 13517–13525.
- Koo, B.H., Goff, C.L., Jungers, K.A., Vasanthi, A., O'Flaherty, J., Weyman, C.M., and Apte, S.S. (2007). ADAMTS-like 2 (ADAMTSL2) is a secreted glycoprotein that is widely expressed during mouse embryogenesis and is regulated during skeletal myogenesis. *Matrix Biol.* 26, 431–441.
- Kostka, G., Giltay, R., Bloch, W., Addicks, K., Timpl, R., Fassler, R., and Chu, M.L. (2001). Perinatal lethality and endothelial cell abnormalities in several vessel compartments of fibulin-1-deficient mice. *Mol. Cell. Biol.* 21, 7025–7034.
- Kubota, Y., Kuroki, R., and Nishiwaki, K. (2004). A fibulin-1 homolog interacts with an ADAM protease that controls cell migration in *C. elegans*. *Curr. Biol.* 14, 2011–2018.
- LaPierre, D.P., Lee, D.Y., Li, S.Z., Xie, Y.Z., Zhong, L., Sheng, W., Deng, Z., and Yang, B.B. (2007). The ability of versican to simultaneously cause apoptotic resistance and sensitivity. *Cancer Res.* 67, 4742–4750.
- Lee, N.V., Rodriguez-Manzanera, J.C., Thai, S.N., Twal, W.O., Luque, A., Lyons, K.M., Argraves, W.S., and Iruela-Arispe, M.L. (2005). Fibulin-1 acts as a cofactor for the matrix metalloprotease ADAMTS-1. *J. Biol. Chem.* 280, 34796–34804.
- Llamazares, M., Cal, S., Quesada, V., and Lopez-Otin, C. (2003). Identification and characterization of ADAMTS-20 defines a novel subfamily of metalloproteinases-disintegrins with multiple thrombospondin-1 repeats and a unique GON domain. *J. Biol. Chem.* 278, 13382–13389.
- Longpre, J.M., McCulloch, D.R., Koo, B.H., Alexander, J.P., Apte, S.S., and Leduc, R. (2009). Characterization of proADAMTS5 processing by proprotein convertases. *Int. J. Biochem. Cell Biol.* 41, 1116–1126.
- Lu, P., Minowada, G., and Martin, G.R. (2006). Increasing Fgf4 expression in the mouse limb bud causes polysyndactyly and rescues the skeletal defects that result from loss of Fgf8 function. *Development* 133, 33–42.
- Matsumoto, K., Shionyu, M., Go, M., Shimizu, K., Shinomura, T., Kimata, K., and Watanabe, H. (2003). Distinct interaction of versican/PG-M with hyaluronan and link protein. *J. Biol. Chem.* 278, 41205–41212.
- McCulloch, D.R., Goff, C.L., Bhatt, S., Dixon, L.J., Sandy, J.D., and Apte, S.S. (2009). Adamts5, the gene encoding a proteoglycan-degrading metalloprotease, is expressed by specific cell lineages during mouse embryonic development and in adult tissues. *Gene Expr. Patterns* 9, 314–323.
- Merino, R., Ganan, Y., Macias, D., Rodriguez-Leon, J., and Hurler, J.M. (1999a). Bone morphogenetic proteins regulate interdigital cell death in the avian embryo. *Ann. N Y Acad. Sci.* 887, 120–132.
- Merino, R., Rodriguez-Leon, J., Macias, D., Ganan, Y., Economides, A.N., and Hurler, J.M. (1999b). The BMP antagonist Gremlin regulates outgrowth, chondrogenesis and programmed cell death in the developing limb. *Development* 126, 5515–5522.

- Mjaatvedt, C.H., Yamamura, H., Capehart, A.A., Turner, D., and Markwald, R.R. (1998). The *Cspg2* gene, disrupted in the *hdf* mutant, is required for right cardiac chamber and endocardial cushion formation. *Dev. Biol.* 202, 56–66.
- Olin, A.I., Morgelin, M., Sasaki, T., Timpl, R., Heinegard, D., and Aspberg, A. (2001). The proteoglycans aggrecan and Versican form networks with fibulin-2 through their lectin domain binding. *J. Biol. Chem.* 276, 1253–1261.
- Pajni-Underwood, S., Wilson, C.P., Elder, C., Mishina, Y., and Lewandoski, M. (2007). BMP signals control limb bud interdigital programmed cell death by regulating FGF signaling. *Development* 134, 2359–2368.
- Perissinotto, D., Iacopetti, P., Bellina, I., Doliana, R., Colombatti, A., Pettway, Z., Bronner-Fraser, M., Shinomura, T., Kimata, K., Morgelin, M., et al. (2000). Avian neural crest cell migration is diversely regulated by the two major hyaluronan-binding proteoglycans PG-M/versican and aggrecan. *Development* 127, 2823–2842.
- Rao, C., Foernzler, D., Loftus, S.K., Liu, S., McPherson, J.D., Jungers, K.A., Apte, S.S., Pavan, W.J., and Beier, D.R. (2003). A defect in a novel ADAMTS family member is the cause of the belted white-spotting mutation. *Development* 130, 4665–4672.
- Russell, D.L., Doyle, K.M., Ochsner, S.A., Sandy, J.D., and Richards, J.S. (2003). Processing and localization of ADAMTS-1 and proteolytic cleavage of versican during cumulus matrix expansion and ovulation. *J. Biol. Chem.* 278, 42330–42339.
- Salas-Vidal, E., Valencia, C., and Covarrubias, L. (2001). Differential tissue growth and patterns of cell death in mouse limb autopod morphogenesis. *Dev. Dyn.* 220, 295–306.
- Sandy, J.D., Westling, J., Kenagy, R.D., Iruela-Arispe, M.L., Verscharen, C., Rodriguez-Mazaneque, J.C., Zimmermann, D.R., Lemire, J.M., Fischer, J.W., Wight, T.N., et al. (2001). Versican V1 proteolysis in human aorta in vivo occurs at the Glu441-Ala442 bond, a site that is cleaved by recombinant ADAMTS-1 and ADAMTS-4. *J. Biol. Chem.* 276, 13372–13378.
- Sasaki, T., Kostka, G., Gohring, W., Wiedemann, H., Mann, K., Chu, M.L., and Timpl, R. (1995). Structural characterization of two variants of fibulin-1 that differ in nidogen affinity. *J. Mol. Biol.* 245, 241–250.
- Silver, D.L., Hou, L., Somerville, R., Young, M.E., Apte, S.S., and Pavan, W.J. (2008). The secreted metalloprotease ADAMTS20 is required for melanoblast survival. *PLoS Genet.* 4, e1000003.
- Somerville, R.P., Longpre, J.M., Jungers, K.A., Engle, J.M., Ross, M., Evanko, S., Wight, T.N., Leduc, R., and Apte, S.S. (2003). Characterization of ADAMTS-9 and ADAMTS-20 as a distinct ADAMTS subfamily related to *Caenorhabditis elegans* GON-1. *J. Biol. Chem.* 278, 9503–9513.
- Stankunas, K., Hang, C.T., Tsun, Z.Y., Chen, H., Lee, N.V., Wu, J.I., Shang, C., Bayle, J.H., Shou, W., Iruela-Arispe, M.L., et al. (2008). Endocardial Brg1 represses ADAMTS1 to maintain the microenvironment for myocardial morphogenesis. *Dev. Cell* 14, 298–311.
- Stanton, H., Rogerson, F.M., East, C.J., Golub, S.B., Lawlor, K.E., Meeker, C.T., Little, C.B., Last, K., Farmer, P.J., Campbell, I.K., et al. (2005). ADAMTS5 is the major aggrecanase in mouse cartilage in vivo and in vitro. *Nature* 434, 648–652.
- Suwan, K., Choocheep, K., Hatano, S., Kongtawelert, P., Kimata, K., and Watanabe, H. (2009). Versican/Pg-M assembles hyaluronan into extracellular matrix and inhibits CD44-mediated signaling toward premature senescence in embryonic fibroblasts. *J. Biol. Chem.* 284, 8596–8604.
- Thai, S.N., and Iruela-Arispe, M.L. (2002). Expression of ADAMTS1 during murine development. *Mech. Dev.* 115, 181–185.
- Weatherbee, S.D., Behringer, R.R., Rasweiler, J.J.4th, and Niswander, L.A. (2006). Interdigital webbing retention in bat wings illustrates genetic changes underlying amniote limb diversification. *Proc. Natl. Acad. Sci. USA* 103, 15103–15107.
- Zhang, H.Y., Chu, M.L., Pan, T.C., Sasaki, T., Timpl, R., and Ekblom, P. (1995). Extracellular matrix protein fibulin-2 is expressed in the embryonic endocardial cushion tissue and is a prominent component of valves in adult heart. *Dev. Biol.* 167, 18–26.
- Zhang, H.Y., Timpl, R., Sasaki, T., Chu, M.L., and Ekblom, P. (1996). Fibulin-1 and fibulin-2 expression during organogenesis in the developing mouse embryo. *Dev. Dyn.* 205, 348–364.
- Zou, H., and Niswander, L. (1996). Requirement for BMP signaling in interdigital apoptosis and scale formation. *Science* 272, 738–741.
- Zuzarte-Luis, V., and Hurler, J.M. (2002). Programmed cell death in the developing limb. *Int. J. Dev. Biol.* 46, 871–876.